

Retrospective reconstruction of high spatial and temporal resolution temperature maps for tissue property determination

N. Todd¹, J. De Bever², U. Vyas³, A. Payne⁴, and D. L. Parker⁵

¹Physics, University of Utah, Salt Lake City, UT, United States, ²Robotics, University of Utah, Salt Lake City, UT, United States, ³Bioengineering, University of Utah, Salt Lake City, UT, United States, ⁴Mechanical Engineering, University of Utah, Salt Lake City, UT, United States, ⁵Radiology, University of Utah, Salt Lake City, UT, United States

INTRODUCTION:

The most common application of MR temperature imaging (MRTI) is monitoring and control of thermal therapies where fast scan time and real-time reconstruction are critical. However, for certain applications, such as tissue property determination or total accumulated thermal dose calculations, retrospectively reconstructed temperature maps are acceptable. For such purposes, we have applied a temporally constrained reconstruction (TCR) method to MRTI. Here, the technique uses the entire dynamic imaging data set and an iterative cost function minimization algorithm to create 3-D temperature maps with moderate spatial resolution (~2mm³), high temporal resolution (~1 sec), and large field of view coverage (~26x16x3cm³). We present the TCR method and applications to retrospective determination of tissue thermal conductivity, ultrasound power deposition, and total accumulated thermal dose.

METHODS:

Temporally Constrained Reconstruction. The TCR algorithm reconstructs artifact-free images, m , from undersampled k-space data, d , by iteratively minimizing a cost function that consists of a data fidelity term and a constraint term¹:

$$m = \arg \min_{m'} \left(\|WFm' - d\|_2^2 + \alpha \sum_i \|\nabla_i m'_i\|_2^2 \right) \quad [1]$$

where F is the Fourier Transform, W is a binary sparsifying function that represents which phase encoding lines have been acquired, m' is the image estimate, and $\|\cdot\|_2$ represents the L₂ norm. In this implementation, the constraint term penalizes abrupt changes in time in the image, weighted by the free parameter α . Using an entire 4-D data set and 50 – 100 iterations, the algorithm takes many minutes to converge to an alias-free image. Because of this computational burden, the method is not suitable for real-time applications.

Experiments. All experiments were performed in an MRgHIFU system consisting of a Siemens TIM Trio 3T scanner, a 256-element phased-array HIFU transducer (Imasonics, inc), and hardware and software for beam steering and data visualization (Image Guided Therapy). HIFU heating was performed on an agar phantom (70W for 28 sec) and monitored with a 3-D segmented EPI gradient echo sequence with parameters: TR/TE = 25/9 ms, 128x81x16 imaging matrix, EPI factor 9, 2.0mm³ isotropic resolution. Undersampled k-space data sets, with readout lines spread throughout k_y-k_z space, were acquired every 0.5 s, and full k-space data sets were acquired every 4.5 s. Images were reconstructed in four ways: using the undersampled k-space data sets in the TCR algorithm with and without zero-filled interpolation (ZFI) (2x in k_x, k_y, and k_z for 1x1x1mm voxel spacing), and using a traditional inverse Fourier transform on the fully sampled k-space data sets with and without ZFI. All temperature maps were created with a reference-less PRF technique².

Retrospective Calculations. The four different temperature maps were used to retrospectively calculate the phantom thermal conductivity³ (k), the ultrasound power deposition field⁴ (Q), and the total thermal dose⁵ (D), using the methods in the cited references.

RESULTS:

Results are summarized in Table 1. For each of the reconstructions, the calculated values for thermal conductivity, power deposition at the hottest voxel, and total accumulated dose for the hottest voxel are displayed. Fig 1 shows a plot of the hottest voxel over time for each of the four reconstructions. Fig 2 shows how the thermal conductivity is calculated using the TCR ZFI temperatures, based on the method of Cheng and Plewes which measures the spreading of the Gaussian-approximated hotspot as it cools. Fig 4 shows the calculation of the deposited power in a single voxel by fitting a line to the initial portion of the TCR ZFI temperature curve of that voxel.

	k (W/m ² °C)	Max Q (W/m ³)	Max D (CEM)
iFFT, 2x2x2 mm, 4.5 s	2.50 e5	5.98 e6	1.96 e4
iFFT, ZFI, 1x1x1 mm, 4.5 s	2.42 e5	8.40 e6	1.78 e5
TCR, 2x2x2 mm, 0.5 s	2.52 e5	6.51 e6	2.03 e4
TCR, ZFI, 1x1x1 mm, 0.5 s	3.33 e5	8.56 e6	2.64 e5

Table 1. Thermal conductivity (k), max power deposition (Q), and max thermal dose (D) values from each temperature map.

DISCUSSION:

Zero-filling to create smaller voxel spacing and using TCR for a smaller time step allows for better tracking of the heating rise and peak temperature. This has a significant impact on how the deposited power and thermal dose are measured. It is less clear whether these attributes affect the measurement of thermal conductivity, which uses information from the cooling portion of the curve.

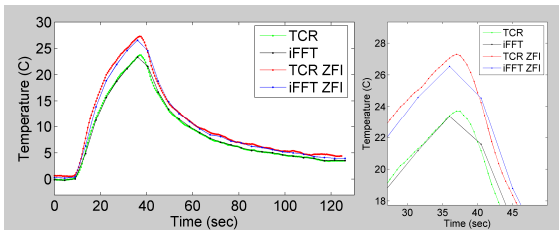


Fig 1. Temperature plots of the hottest voxel for each of the 4 temperature reconstructions, with zoom in on the peak heating.

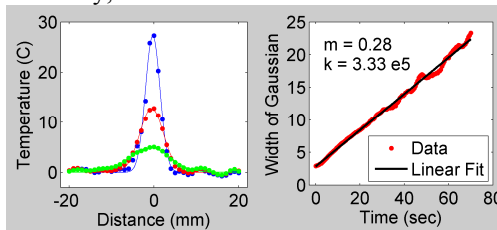


Fig 2. Thermal conductivity determination using TCR ZFI temperatures with 0.5 s temporal resolution and 1x1x1mm voxel spacing.

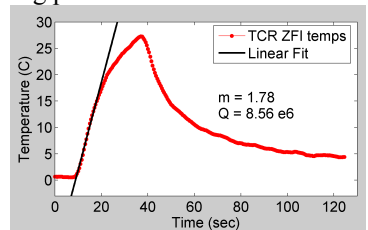


Fig 3. Power deposition determination for one voxel using TCR ZFI temperatures.

REFERENCES: 1. Todd. MRM 2009; 62:406 – 419. 2. Rieke. MRM 2004; 51(6):1223-1231. 3. Cheng. JMRI 2002;16(5):598-609. 4. Roemer. Int J Radiat Oncol Biol Phys 1985;11(8):1539-1550. 5. Sapareto. Int J Radiat Oncol Biol Phys 1984;10(6):787-800.

ACKNOWLEDGEMENTS: This work was supported by The Margolis Foundation, Siemens Medical Solutions, NIH grants F31 EB007892-01A1, R01 CA87785, and R01 CA134599.